

The effect of pressure on the structural properties of the spin-tetrahedra compound
 $\text{Cu}_2\text{Te}_2\text{O}_5\text{Br}_2$

This article has been downloaded from IOPscience. Please scroll down to see the full text article.

2005 J. Phys.: Condens. Matter 17 S807

(<http://iopscience.iop.org/0953-8984/17/11/010>)

View [the table of contents for this issue](#), or go to the [journal homepage](#) for more

Download details:

IP Address: 129.252.86.83

The article was downloaded on 27/05/2010 at 20:30

Please note that [terms and conditions apply](#).

The effect of pressure on the structural properties of the spin-tetrahedra compound $\text{Cu}_2\text{Te}_2\text{O}_5\text{Br}_2$

X Wang¹, I Loa¹, K Syassen^{1,4}, P Lemmens¹, M Hanfland² and M Johansson³

¹ Max-Planck-Institut für Festkörperforschung, Heisenbergstrasse 1, D-70569 Stuttgart, Germany

² European Synchrotron Radiation Facility, BP 220, F-38043 Grenoble, France

³ Department of Inorganic Chemistry, Stockholm University, S-10691 Stockholm, Sweden

E-mail: k.syassen@fkf.mpg.de

Received 12 January 2005

Published 4 March 2005

Online at stacks.iop.org/JPhysCM/17/S807

Abstract

The structural properties of the spin-tetrahedra compound $\text{Cu}_2\text{Te}_2\text{O}_5\text{Br}_2$ have been investigated under hydrostatic pressure up to 24 GPa by angle-dispersive x-ray powder diffraction using synchrotron radiation. The tetragonal phase ($P\bar{4}$, $Z = 2$) remains stable up to about 14 GPa where a reversible structural phase transition takes place. A monoclinic unit cell is assigned to the high-pressure phase. Refinements of atomic positions have been performed for the low-pressure tetragonal phase. The obtained changes in bond lengths and angles provide valuable information for a modelling of the magnetic couplings in this system under pressure.

1. Introduction

Low-dimensional quantum magnetism is receiving considerable attention nowadays. Reduced dimensionality of a quantum spin system in combination with frustration of antiferromagnetic exchange may lead to unconventional ground state properties and magnetic phase diagrams. Attempts to synthesize new low-dimensional quantum spin systems led to the discovery of the compounds $\text{Cu}_2\text{Te}_2\text{O}_5\text{X}_2$ ($\text{X} = \text{Cl}, \text{Br}$) [1]. These represent a new class of cluster compounds with tetrahedral (i.e. frustrated) intra-cluster arrangement of $S = 1/2$ spins and weak coupling between spin tetrahedra.

The $\text{Cu}_2\text{Te}_2\text{O}_5\text{X}_2$ ($\text{X} = \text{Cl}, \text{Br}$) compounds crystallize in the non-centrosymmetric tetragonal space group $P\bar{4}$ with $Z = 2$ formula units per cell. Layers of cluster units $\text{Cu}_4\text{O}_4\text{X}_4$ are stacked along the c -direction and are separated by lone-pair Te atoms (figure 1). The four Cu^{2+} ions within a cluster form a tetrahedron. Bridging ligand oxygens provide a non-collinear superexchange path $\text{Cu}-\text{O}-\text{Cu}$ between neighbouring Cu^{2+} ions.

⁴ Author to whom any correspondence should be addressed.

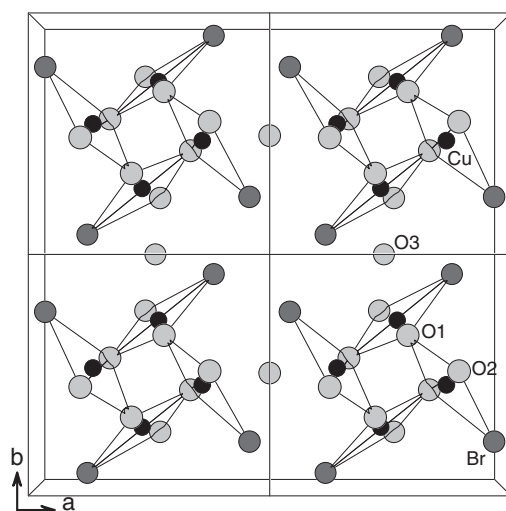


Figure 1. Projection of the tetragonal crystal structure of $\text{Cu}_2\text{Te}_2\text{O}_5\text{Br}_2$ along the c -axis. Four unit cells are shown. For clarity, Te atoms are not shown.

Several low-temperature experimental studies of magnetic properties and Raman-active excitations have revealed unusual behaviours [1–6]. The nature of the ordered states remains unsettled at the microscopic level. $\text{Cu}_2\text{Te}_2\text{O}_5\text{Br}_2$ has been suggested to be close to a quantum critical point. Theoretical work has addressed the intra-tetrahedral exchange couplings as well as the inter-tetrahedral ones [3, 7–14]. The latter are realized by ‘super-super-exchange’ paths between adjacent $\text{Cu}_4\text{O}_8\text{Br}_4$ clusters via $\text{Cu}-\text{Br} \cdots \text{Br}-\text{Cu}$ and $\text{Cu}-\text{O} \cdots \text{O}-\text{Cu}$ paths.

Pressure experiments are a particularly useful tool for tuning interatomic interactions. We report here the effects of hydrostatic pressure on the structural properties of $\text{Cu}_2\text{Te}_2\text{O}_5\text{Br}_2$ as probed by angle-dispersive powder x-ray diffraction using synchrotron radiation. Our main interest is in pressure-induced changes of internal structural parameters in the *tetragonal* phase. Such structural details are highly relevant for an interpretation of pressure effects on magnetic interactions as probed by, for example, Raman scattering [5] or by magnetic susceptibility measurements [6] under pressure. A second aspect is the structural phase stability under pressure. We find the tetragonal phase to exist up to about 14 GPa (300 K). Near this pressure, the structure starts to distort. We assign a monoclinic unit cell to the high-pressure phase.

2. Experimental details

The preparation of $\text{Cu}_2\text{Te}_2\text{O}_5\text{Br}_2$ single crystals available for this study is reported elsewhere [1]. A small crystal was ground to a fine powder, and the powder was loaded into a diamond anvil cell (DAC). Nitrogen was chosen as the pressure medium in order to produce nearly hydrostatic pressure conditions. Angle-dispersive powder x-ray diffraction patterns (wavelength $\lambda = 0.4176 \text{ \AA}$) were measured at the ID9 beamline of the European Synchrotron Radiation Facility, Grenoble, using image plate detection. The images were integrated using the FIT2D software [15] to yield one-dimensional intensity versus 2θ diagrams. The instrumental resolution, i.e. the minimum full width at half maximum (FWHM) of the diffraction peaks, was about 0.04° . To improve powder averaging, the DAC was rotated by $\pm 3^\circ$ during exposure. The ruby luminescence method was used for pressure determination [16, 17].

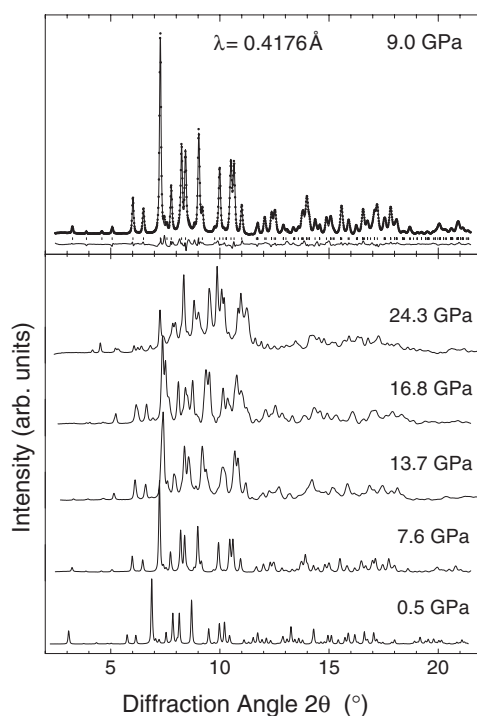


Figure 2. Diffraction patterns of $\text{Cu}_2\text{Te}_2\text{O}_5\text{Br}_2$ at selected pressures ($T = 300$ K). A smooth background arising mainly from Compton scattering in the diamond anvils is subtracted from all diagrams. The tetragonal phase ($P4$, $Z = 2$) remains stable up to about 14 GPa. An example of a full Rietveld refinement of high-pressure data (9.0 GPa, tetragonal phase) is shown in the top frame. The diagrams indicate the occurrence of a structural phase transition near 14 GPa. A monoclinic unit cell is assigned to the high-pressure phase.

3. Results and discussion

Selected diffraction patterns of $\text{Cu}_2\text{Te}_2\text{O}_5\text{Br}_2$ at different pressures are presented in figure 2. The tetragonal low-pressure phase is observed up to 13.7 GPa. Diffraction patterns for this phase were suitable for refinements of the lattice parameters as well as the atomic positions. The full Rietveld refinements were performed using GSAS [18]. Results for atomic positions are considered further below.

Subtle changes can be detected in the diagrams taken just above 14 GPa and more obvious peak splittings occur at higher pressure. These observations indicate a phase transition starting near 14 GPa. Furthermore, the subtle changes across the phase transition pressure indicate that the high-pressure phase is a distorted variant of the tetragonal phase. With this in mind, the diffraction diagrams of the high-pressure phase have been indexed in the monoclinic system (using the DICVOL program [19]). The obtained monoclinic cell involves a doubling of the original tetragonal cell along its c -axis, an orthorhombic distortion, and a rather small deviation of the monoclinic angle from 90° .

Unit cell parameters of the low- and high-pressure phases of $\text{Cu}_2\text{Te}_2\text{O}_5\text{Br}_2$ as a function of pressure are shown in figure 3. In the tetragonal phase, the a -axis is more compressible compared to the c -axis, at least at low pressures. As a result the c/a -ratio increases in a sub-linear manner; the total change of c/a amounts to about 4% between 0 and 13 GPa. In

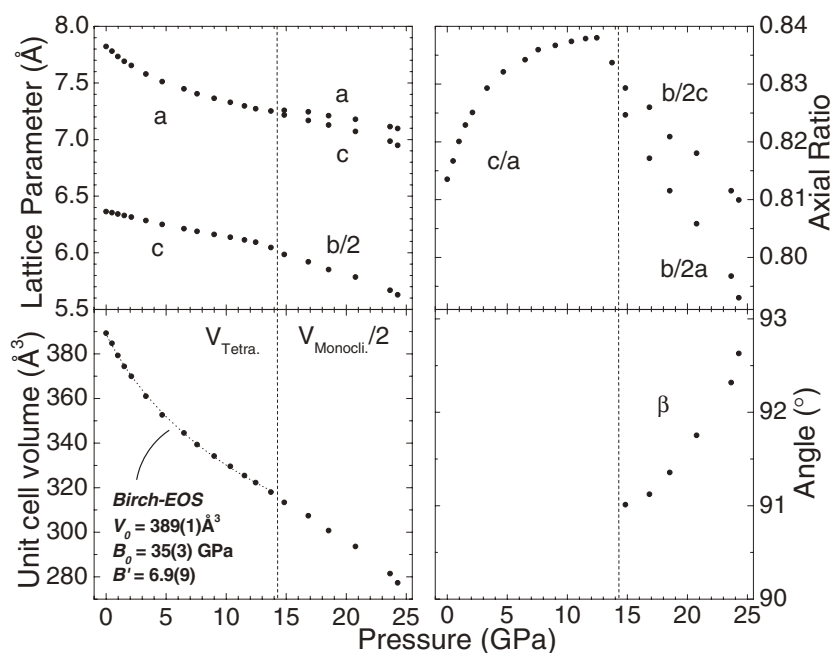


Figure 3. Unit cell parameters and volume of $\text{Cu}_2\text{Te}_2\text{O}_5\text{Br}_2$ as a function of pressure. Dashed vertical lines mark the phase transition from tetragonal to monoclinic. The b -axis and the volume of the high-pressure phase ($Z = 4$) are scaled by a factor of two in order to allow for a direct comparison with the corresponding data for the tetragonal phase ($Z = 2$).

the monoclinic phase, the axial ratios $b/2a$ and $b/2c$ (corresponding to the tetragonal c/a) decrease with increasing pressure. This trend correlates with an increase of the monoclinic angle. Figure 3 also shows the unit cell volume as a function of pressure. For the small volume decrease across the phase boundary, if any, we can only give an upper limit of -0.3% . A fit of a Birch equation of state to the PV data of the tetragonal phase gives, using $V_0 = 389.3 \text{ \AA}^3$, the values of bulk modulus $B_0 = 35(3) \text{ GPa}$ and the pressure derivative of the bulk modulus $B'_0 = 6.9(9)$.

We now turn to the pressure dependence of the internal structural parameters of tetragonal $\text{Cu}_2\text{Te}_2\text{O}_5\text{Br}_2$. As mentioned, the Rietveld refinements were performed using GSAS [18]. Thermal parameters were fixed at the values given in [1]. A small correction for preferred orientation had to be taken into account. As an example, the top part of figure 2 shows the result of the profile refinement of tetragonal $\text{Cu}_2\text{Te}_2\text{O}_5\text{Br}_2$ ($P4$, $Z = 2$) at 9.0 GPa. In this case the convergence was achieved (with a subtracted background) at a residual $R_{\text{wp}} = 7.2\%$. Numerical results from refinements for ambient pressure and for 9 GPa are summarized in table 1.

The refinement strategy requires a comment. At high pressures, all positions except those of O2 were refined. The reason is that the O2 position was identified to cause a redundant-parameter problem. With the constraint of fixed O2 positions, we are left with 13 positional parameters. Based on our diffraction diagrams at ambient, the published crystallographic (single-crystal) data [1] are essentially reproduced. Even the O1 and O3 positions come out in reasonable agreement. Furthermore, under pressure all nearest-neighbour distances change in a plausible manner (cf figure 4). In particular, the obtained large change of the Br–Br distance (an important piece of information here) is not in conflict with what is known about compressed bromine itself. So, we can have confidence in the results obtained from the refinements.

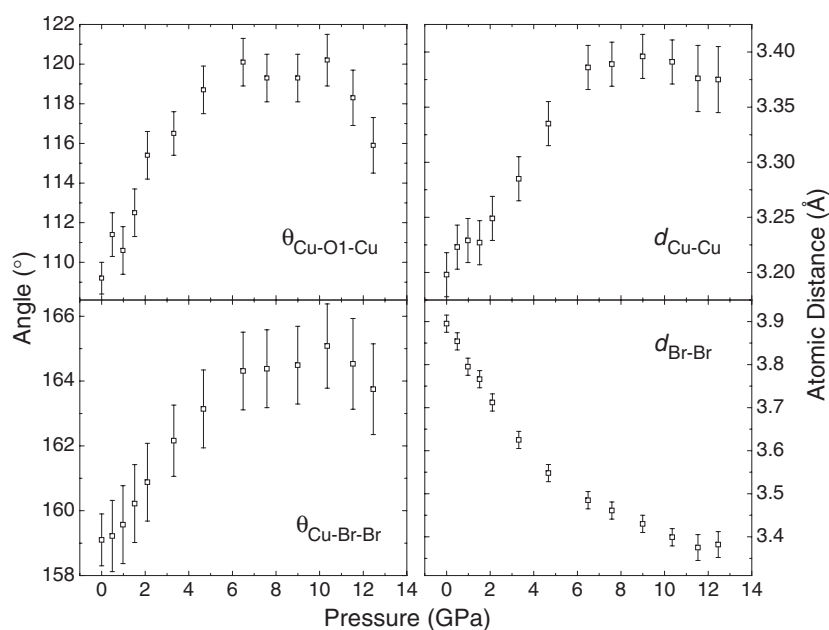


Figure 4. Selected bond lengths and bond angles of the tetragonal phase of $\text{Cu}_2\text{Te}_2\text{O}_5\text{Br}_2$ as a function of pressure. Note the large decrease of the inter-cluster Br–Br distance.

Table 1. Structural parameters obtained from Rietveld refinements of diffraction diagrams for $\text{Cu}_2\text{Te}_2\text{O}_5\text{Br}_2$ at 300 K. The space group is $P\bar{4}$ ($Z = 2$). The top part refers to data taken at 0 GPa ($a = 7.8217 \text{ \AA}$, $c = 6.3633 \text{ \AA}$, $V = 389.3 \text{ \AA}^3$, $R_{\text{wp}} = 5.7\%$), the bottom part to 9 GPa ($a = 7.3642 \text{ \AA}$, $c = 6.1616 \text{ \AA}$, $V = 334.16 \text{ \AA}^3$, $R_{\text{wp}} = 7.2\%$). Realistic relative errors for the lattice parameters are 2×10^{-4} . The uncertainties stated below are the estimated standard deviations reported by the refinement software GSAS. Parameters marked by an asterisk are not refined (see the text for comments).

	Atom	Site	x	y	z
0 GPa	Te	4h	0.6387(1)	0.8187(1)	0.3605(1)
	Cu	4h	0.7238(1)	0.4657(1)	0.1563(2)
	Br	4h	0.9172(1)	0.2348(1)	0.1823(1)
	O1	4h	0.5667(4)	0.6682(5)	0.1340(7)
	O2	4h	0.4684(3)	0.7590(3)	0.5558(4)
	O3	2g	0.5	0	0.2362(4)
9 GPa	Te	4h	0.6548(4)	0.8348(5)	0.3532(4)
	Cu	4h	0.7346(8)	0.4524(7)	0.1671(12)
	Br	4h	0.9196(6)	0.2040(5)	0.1877(8)
	O1	4h	0.5862(24)	0.6550(33)	0.1181(38)
	O2	4h	0.4684*	0.7590*	0.5558*
	O3	2g	0.5	0	0.2114(26)

In the top two frames of figure 4 we present the pressure dependence of parameters associated with intra-tetrahedral couplings, and the bottom frames illustrate the corresponding geometrical parameters important for inter-tetrahedral couplings. The bond changes are quite pronounced with increasing pressures. In particular, we find a large decrease of the Br–Br distance at high pressures. At ambient pressure, this distance (3.895 Å) is close to the van der

Waals distance (3.9 Å). At 11.5 GPa the Br–Br distance decreases to 3.375 Å, i.e. it shrinks by 13%. Consequently, the Cu–Br ··· Br–Cu exchange paths may provide much stronger exchange interactions under pressure. Pressure-enhanced inter-cluster couplings may account for the observed large changes in the magnetic scattering channel seen in low-temperature Raman spectra, i.e. the disappearance of the longitudinal magnon at 1 GPa and an extremely large shift of the 2-magnon-like continuum to higher energies [5].

To summarize, we have investigated the structural properties of $\text{Cu}_2\text{Te}_2\text{O}_5\text{Br}_2$ at high pressures up to 24 GPa. A new high-pressure phase has been observed above 14 GPa and it was identified to be a monoclinically distorted variant of the tetragonal phase. Unit cell parameters as a function of pressure are reported for the tetragonal and monoclinic phases. Furthermore, the pressure dependences of the atomic positions of the low-pressure tetragonal phase have been obtained by Rietveld refinements. The latter results are considered valuable information for the interpretation of the magnetic properties and magnetic excitations of $\text{Cu}_2\text{Te}_2\text{O}_5\text{Br}_2$ under pressure.

References

- [1] Johnsson M, Törnroos K W, Mila F and Millet P 2000 *Chem. Mater.* **12** 2853
- [2] Lemmens P, Choi K-Y, Kaul E E, Geibel C, Becker K, Brenig W, Valenti R, Gros C, Johnsson M, Millet P and Mila F 2001 *Phys. Rev. Lett.* **87** 227201
- [3] Gros C, Lemmens P, Vojta M, Valenti R, Choi K-Y, Kageyama H, Hiroi Z, Mushnikov N V, Goto T, Johnsson M and Millet P 2003 *Phys. Rev. B* **67** 174405
- [4] Prester M, Smontara A, Zivkovic I, Bilusic A, Drobac D, Berger H and Bussy F 2004 *Phys. Rev. B* **69** 180401
- [5] Wang X, Loa I and Syassen K, unpublished
- [6] Kreitlow J, Süllow S, Menzel D, Schoenes J, Lemmens P and Johnsson M 2005 *J. Magn. Magn. Mater.* at press
- [7] Brenig W and Becker K W 2001 *Phys. Rev. B* **64** 214413
- [8] Kotov V N, Yhitomirsky M E and Sushkov O P 2001 *Phys. Rev. B* **63** 064412
- [9] Valenti R, Saha-Dasgupta T and Gros C 2002 *Phys. Rev. B* **66** 054426
- [10] Totsuka K and Mikeska H J 2002 *Phys. Rev. B* **66** 054435
- [11] Valenti R, Saha-Dasgupta T, Gros C and Rosner H 2003 *Phys. Rev. B* **67** 245110
- [12] Brenig W 2003 *Phys. Rev. B* **67** 064402
- [13] Jensen J, Lemmens P and Gros C 2003 *Europhys. Lett.* **64** 689
- [14] Whangbo M-H, Koo H-J and Dai D 2003 *Inorg. Chem.* **42** 3898
- [15] Hammersley A P, Svensson S O, Hanfland M, Fitch A N and Häussermann D 1996 *High Pressure Res.* **14** 235
- [16] Piermarini G J, Block S, Barnett J D and Forman R A 1975 *J. Appl. Phys.* **46** 2774
- [17] Mao H K, Xu J and Bell P M 1986 *J. Geophys. Res.* **91** 4673
- [18] Larson A C and van Dreele R B 2000 GSAS: general structure analysis system *Los Alamos National Laboratory Report LAUR 86-748*
- [19] Boulton A and Louer D 1991 *J. Appl. Crystallogr.* **24** 987